BIFURCATING SOLUTIONS OF THE FLOW INDUCED BY A FREE ROTATING IMPELLER OF A HIGH PRESSURE FAN

Andrei DRAGOMIRESCU[1], Valeriu Nicolae PANAITESCU[2]

This paper presents a study of the turbulent, compressible air flow induced by an impeller of a high pressure fan. The equations governing the flow – continuity equation, Reynolds-averaged Navier-Stokes equations, energy equation and the equation of state – were solved using the finite volume method. The Reynolds stress model was used to provide the closure equations. Different overpressures were imposed as boundary conditions at the outflow for each simulation. The overpressures were varied stepwise between the choke limit and the limit corresponding to reversed flow. The results obtained indicate the appearance of two bifurcating solutions at certain operating points. These solutions are characterized by two and, respectively, three dominant directions of the flow outside the impeller. By dominant directions we denote regions where the velocity is higher than in neighbouring areas at the same radius. Based on the results, a bifurcation diagram is presented. The bifurcating solutions seem not to affect the performance of the impeller.

Keywords: bifurcating solutions, compressible flow, high pressure fan, free impeller.

1. Introduction

Gas flows through high pressure fans, i.e. fans having compression ratios between 1.036 and 1.3 according to Eurovent norms [1], should be treated as compressible, otherwise errors in the fan discharge up to 15% are to be expected, as inferred by Dragomirescu and Panaitescu [2]. Compressible turbulent flows induced by impellers are governed by the equation of state and several partial differential equations: continuity equation, momentum equation, energy equation and the equations corresponding to the turbulence model chosen to study the flow. Due to the movement of the fan impeller, the gas flow is inherently unsteady, so that the governing partial differential equations can be written in the following condensed form:

$$\frac{\mathrm{d}\mathbf{U}}{\mathrm{d}t} = \mathbf{F}(\mu, \mathbf{U}), \tag{1}$$

with the initial value

$$\mathbf{U}(0) = \mathbf{U}_0 \tag{2}$$

and associated boundary conditions. In the above equations **U** is the vector of flow

[1] Lecturer, Faculty of Power Engineering, University "Politehnica" of Bucharest, Romania
[2] Prof. PhD., Faculty of Power Engineering, University "Politehnica" of Bucharest, Romania

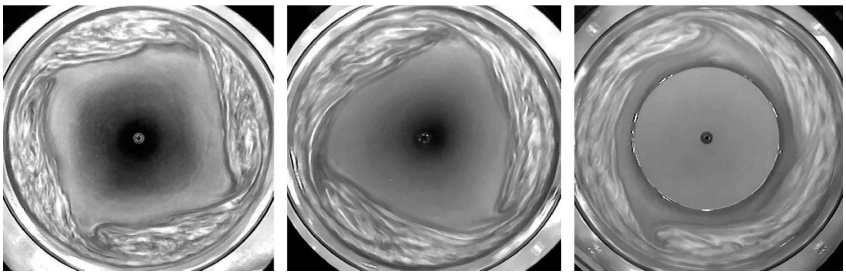

Fig. 1. Flow configurations induced by a disc rotating inside a casing, observed by Poncet and Chauve [8]

variables (velocity components, pressure, temperature, density, turbulent variables), **F** is a vector function whose components are functions of the components of **U**, and μ is a vector of parameters (gas viscosity, thermal diffusivity, etc.). A solution to which equation (1) evolves after the transient effects associated with the initial values (2) have diminished is called *asymptotic solution*. It should be mentioned here that $\mathbf{U} = 0$ cannot be a solution to the problem, since $\mathbf{U} \neq 0$ is forced by nonzero forcing data embedded in $\mathbf{F}(\mu, \mathbf{U})$, and, if applicable, in the boundary conditions. Examples of nonzero forcing data are the pressure force per unit mass, $1/\rho \nabla p$, and, in a non-inertial reference frame attached to the impeller, the centrifugal force per unit mass, $\boldsymbol{\omega} \times (\boldsymbol{\omega} \times \mathbf{r})$. Among the possible asymptotic solutions of the autonomous problem formulated above there are (i) steady solutions and (ii) T-periodic solutions of the form $\mathbf{U}(t) = \mathbf{U}(t + T)$. Asymptotic solutions which form intersecting branches in a suitable space of functions are called *bifurcating solutions*. It is said that one asymptotic solution bifurcates from another at $\mu = \mu_0$ if there are two distinct asymptotic solutions $\mathbf{U}^{(1)}(\mu_0, t)$ and $\mathbf{U}^{(2)}(\mu_0, t)$, continuous in μ, such that $\mathbf{U}^{(1)}(\mu_0, t) = \mathbf{U}^{(2)}(\mu_0, t)$. One work, in which the bifurcation theory is extensively treated, is that of Ioos and Joseph [3].

An important characteristic of bifurcation is the appearance of solutions that can break the symmetry pattern of the forcing data, should this symmetry exists. Thus, non-symmetrical solutions are also possible when the geometry and the boundary conditions are symmetrical. Bifurcating solutions were found experimentally and numerically even in cases of simple flows, like those through symmetrical sudden expansions [4, 5], through a symmetrical channel with a sudden expansion and a sudden contraction [6], or through a lid driven cavity with throughflow [7]. More recently, Poncet and Chauve [8] identified different flow configurations, without axial symmetry, of the flow induced by a disc rotating inside a casing. Three such configurations are presented in Figure 1.

It is often true that a necessary condition for bifurcation is the instability of the asymptotic solution to small disturbances. In a real flow, disturbances are usually small deviations in the symmetry of the geometry, changes in the

upstream or downstream flow conditions, etc. In a numerical simulation, disturbances can be introduced by the inherent numerical errors.

This paper presents results of numerical simulations performed for the compressible turbulent flow induced by a free impeller of a high pressure fan. The results suggest that, depending on the boundary conditions, one or two non-axisymmetrical flow configurations are possible outside the impeller.

2. Problem description

The study was performed with the commercial code Fluent. Numerical simulations were performed for the impeller of a high pressure fan designed for a rated compression ratio of $\tau = 1.3$. The design was based on a method proposed by Pfleiderer and Petermann [9]. In many cases, in order to keep the machine as simple as possible, fan impellers have a constant width from inlet to outlet. For this reason we chose to use a two-dimensional geometry in our study. The computational domain consists of the impeller and two annular zones placed inside and outside the impeller. A sketch of a part of the computational domain, comprising the impeller, is presented in Figure 2. The diameter at impeller inlet is $D_1 = 330$ mm, while at outlet the diameter is $D_2 = 660$ mm. The impeller has 20 blades shaped as circular arcs of radius $R_b = 296$ mm and having the angles $\beta_1 = 33.5°$ at inlet and $\beta_2 = 90°$ at outlet. The inflow boundary is situated at diameter $D_0 = 0.6 \cdot D_1 = 198$ mm while the outflow boundary (not visible in Figure 2) lies at diameter $D_3 = 3 \cdot D_2 = 2040$ mm. The working fluid is air.

The rotational movement of the impeller renders the flow unsteady, thus the integration of the flow equations being required not only in space but also in time. To catch the effect of the impeller movement on the flow as accurate as possible, the sliding mesh technique was used in the simulations. The

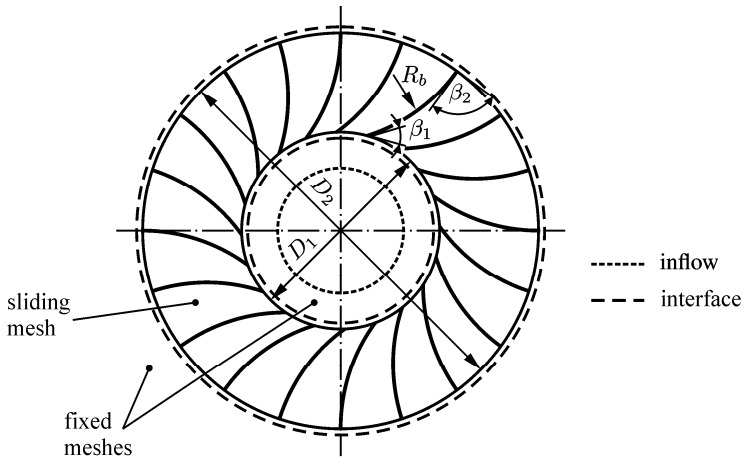

Fig. 2. Impeller sketch and computational domain

computational domain was discretized using three distinct meshes: one moving mesh for the impeller and two fixed meshes for the inflow and outflow annular zones. These meshes are separated by special interfaces that allow the transport of the flow quantities from one mesh to another. A detailed description of the treatment of these interfaces is presented in literature [10]. The nodes of the moving mesh rotate from one time step to another with the angular velocity of the impeller, $\omega = 523.6$ rad/s, which corresponds to a rotational speed of 5000 rpm. All three meshes are unstructured. The mesh attached to impeller was refined close to the blades and especially close to their suction and pressure edges.

The reference pressure and the reference absolute temperature were chosen as $p_0 = 10^5$ Pa and $T_0 = 300$ K, respectively. The required properties of air – dynamic viscosity, specific heat at constant pressure, and thermal conductivity – were input as piece-wise linear functions of temperature using data found in literature [11]. As boundary conditions, the relative total pressure $p_{t0} = 0$ Pa and the absolute temperature $T_0 = 300$ K were set at inflow. The no-slip condition was imposed on the blades. Simulations were performed for relative static pressures at outflow, p_r, ranging from 16000 Pa to 34000 Pa. The numerical simulations were performed by means of the coupled algorithm. Turbulence was modeled using the Reynolds Stress Model, which is considered to be more accurate than other turbulence models when simulating turbomachinery flows [10]. A second order upwind scheme was used to discretize the flow variables, except the turbulent quantities, which were discretized using a first order upwind scheme.

The first simulation was performed for an outflow pressure of 20000 Pa. The initial guess for this simulation was obtained through auxiliary computations, in which the flow was considered laminar, in order to save computing time, and the rotational speed of the impeller and the outflow static pressure were increased stepwise, starting from values close to zero. The solution of the last time step of the simulation at $p_r = 20000$ Pa was then used as initial guess for the next simulation. For each new simulation the outflow static pressure was increased or decreased, as appropriate, by 1000 Pa. As initial guess the final solution obtained for the previous outflow static pressure was used. At each value of the outflow static pressure the simulations were advanced in time with the time step $\Delta t = 0.00015$ s until a stabilization of the flow rate around an average value was observed over 40 revolutions of the impeller.

Simulations were attempted also for outflow static pressures outside the range 16000…34000 Pa, but the results suggested that pressures below 16000 Pa led to choke, while pressures above 34000 Pa caused a reversed flow through the impeller.

3. Results and discussion

The results obtained for $p_r = 20000$ Pa indicate that outside the impeller the flow is not axisymmetrical, as expected, but it shows three regions of higher

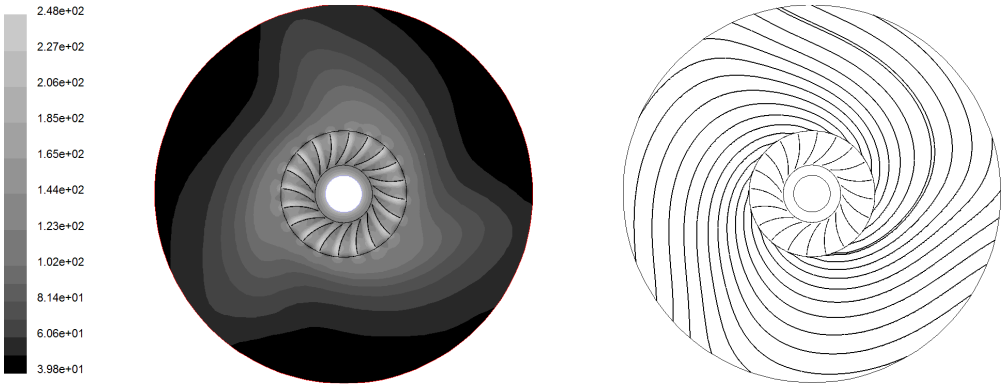

a) b)

Fig. 3. Contours of absolute velocity in m/s (a) and streamlines (b) obtained for an outflow static pressure p_r = 24000 Pa, showing three dominant flow directions

velocity. We will denote further these regions as dominant flow directions. Subsequent simulations showed that this flow configuration kept on reappearing for p_r values in the range 16000…24000 Pa, as long as the simulations were continued from the configuration with three dominant directions obtained at p_r = 20000 Pa. Figure 3 shows contours of absolute velocity and streamlines plotted outside the impeller, which make evident the dominant flow directions. It can be seen that the three directions are practically equally spaced at angles of 120°, the flow possessing a three-fold rotational symmetry with respect to impeller axis.

The image of the flow induced by the impeller changed after the outflow static pressure was increased from 24000 Pa to 25000 Pa and the flow rate became stable. The three dominant directions were replaced by only two dominant directions. As the outflow static pressure was further increased, this flow configuration remained unchanged up to p_r = 29000 Pa.

For values of p_r between 30000 Pa and 32000 Pa the three dominant directions reappeared. Finally, close to the limit of reversed flow, at p_r =33000 Pa and p_r = 34000 Pa the results indicated again flow configurations with only two dominant directions.

The first set of results described above indicate flow configurations which change from three dominant flow directions to two directions and from two directions to three directions, depending on the working regime of the impeller, determined by the outflow static pressure p_r. To check these results, the simulations were repeated starting from the case with the outflow static pressure of 34000 Pa and decreasing p_r stepwise by 1000 Pa. Down to p_r = 25000 Pa, the new results showed no change in the flow configurations by comparison with those obtained previously. A change appeared only when p_r was decreased below

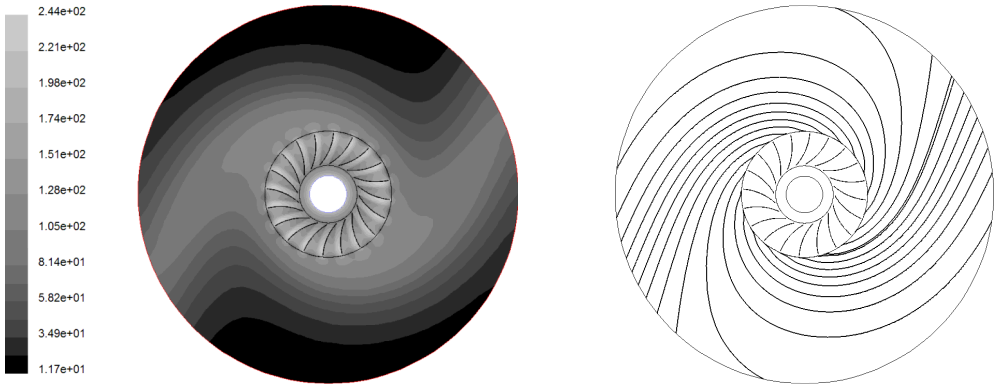

a) b)

Fig. 4. Contours of absolute velocity in m/s (a) and streamlines (b) obtained for an outflow static pressure p_r = 24000 Pa, showing two dominant flow directions

25000 Pa to 24000 Pa, in the sense that instead of observing a switch from two dominant directions to three directions, as expected based on the previous results, the flow preserved its two dominant directions down to p_r = 16000 Pa. In other words, when decreasing the outflow static pressure below 30000 Pa in small steps only flow configurations with two dominant directions can be obtained. Such a flow configuration obtained for p_r = 24000 Pa is presented in Figure 4. With the two dominant directions spaced at 180° the flow possesses a two-fold rotational symmetry with respect to impeller axis.

The new set of results suggests that below p_r = 25000 two flow configurations are possible: either with two or with tree dominant directions. Furthermore, the variation in time of the mass flow rate at outflow changes depending on the flow configuration. Figure 5 shows the time variations of the mass flow rate Q_m when p_r = 24000 Pa. It can be seen that when the flow has two dominant directions the mass flow rate has two modes of oscillation. For three dominant directions a closer look at the local peaks of the mass flow rate variation suggests that more than two modes of oscillation exist.

A third set of results was obtained by increasing the outflow static pressure starting from the solution showing two dominant flow directions obtained for p_r = 16000 Pa in the second set of simulations. This time, the flow configuration remained unchanged, with two directions, up to p_r = 29000 Pa.

The fact that below p_r = 25000 Pa two flow configurations are possible means that a bifurcation point exists between p_r = 24000 Pa and p_r = 25000 Pa. The results presented above are summarized in the form of a bifurcation diagram in Figure 6. The diagram shows the number of flow directions, m, depending on the outflow static pressure p_r. According to the results, the branch corresponding to m = 2 can be traversed in both directions as long as the outflow static pressure

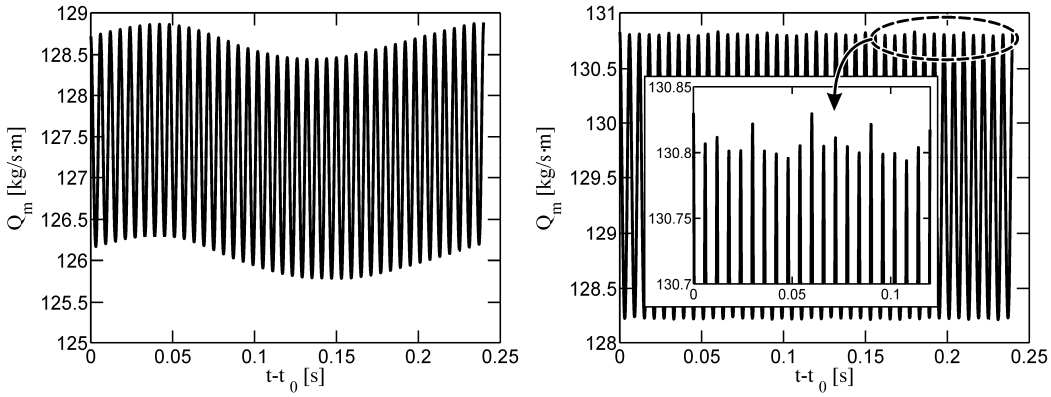

Fig. 5. Mass flow rate variations at outflow over 1600 time steps (20 full rotations) resulted at p_r = 24000 Pa when the flow shows a) two dominant directions and b) three dominant directions

changes in small steps. If only small pressure changes are applied, close to the bifurcation point flow configurations with tree dominant directions evolve in flow configurations with two directions but flow configurations with two directions cannot evolve in flow configurations with three directions.

The performance of the impeller expressed in terms of pressure rise depending on mass flow rate seems not to be affected by the bifurcation. Figure 7 shows that, regardless the flow outside the impeller has two or three dominant directions, all the operating points obtained by numerical simulations lie on the same curve. The only visible effect is a shift of the operating points along the curve depending on the number of dominant directions.

4. Conclusions

In this paper results of a numerical study on the compressible turbulent flow induced by the free impeller of a high pressure fan were presented. For modeling the turbulence the Reynolds Stress Model was chosen. The equations governing the flow were integrated using the finite volume method implemented in the commercial code Fluent. Different operating points were simulated by changing stepwise the outflow static pressure between 16000 Pa and 34000 Pa.

The results obtained indicate that the flow outside the impeller is not axisymmetrical but has either two or three regions of higher velocities, denoted as dominant flow directions. For outflow static pressures of 24000 Pa and below, both flow configurations appeared, while for 25000 Pa and above only one configuration was obtained. This means that at a value of the outflow static pressure comprised between 24000 Pa and 25000 Pa a bifurcation of the flow solution appears. A bifurcation diagram was plotted based on the results.

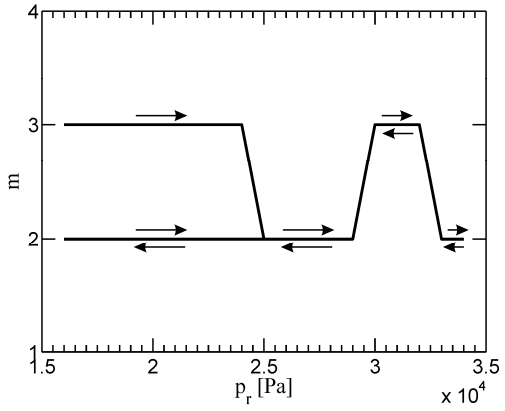

Fig. 6. Bifurcation diagram

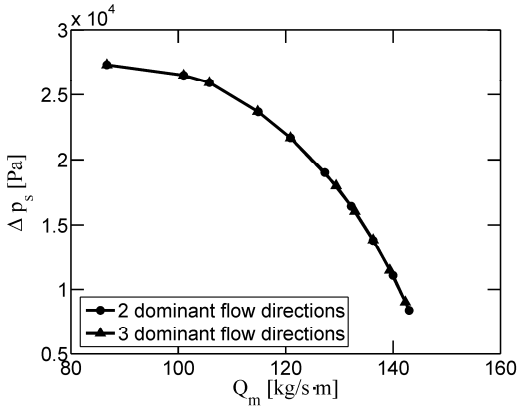

Fig. 7. Impeller performance

Acknowledgements

The authors would like to gratefully acknowledge the financial support provided by the Romanian agency UEFISCSU through the research grant ID 778, which allowed carrying out this study.

R E F E R E N C E S

[1]. *** Eurovent 1/1 – Fan Terminology, EUROVENT/CECOMAF, 1984.
[2]. *A. Dragomirescu, V.N. Panaitescu,* "Assessment of the errors due to neglecting air compressibility when designing fans", in University Politehnica of Bucharest Scientific Bulletin, Series D: Mechanical Engineering, **vol. 70**, 2008, pp. 167-172.
[3]. *G. Iooss, D.D. Joseph,* Elementary stability and bifurcation theory, 2nd Edition, Springer-Verlag, New York, 1990.
[4]. *W. Cherdron, F. Durst, J.H. Whitelaw,* "Asymmetric flows and instabilities in symmetric ducts with sudden expansion", in Journal of Fluid Mechanics, **vol. 84**, 1978, pp.13-31.
[5]. *R.M. Fearn, T. Mullin, K.A. Cliffe,* "Nonlinear flow phenomena in a symmetric sudden expansion", in Journal of Fluid Mechanics, **vol. 211**, 1990, pp. 595-608.
[6]. *J. Mitzushima, Y. Shiotani,* "Transitions and instabilities of flow in a symmetric channel with a suddenly expanded and contracted part", in Journal of Fluid Mechanics, **vol. 434**, 2001, pp. 355-369.
[7]. *A. Dragomirescu,* "Flow configurations in a lid driven cavity with throughflow", in University Politehnica of Bucharest Scientific Bulletin, Series D: Mechanical Engineering, **vol. 66**, no. 2-4, 2004, pp. 137-148.
[8]. *S. Poncet, M.-P. Chauve,* "Shear-layer instability in a rotating system", in Journal of Flow Visualization and Image Processing, **vol. 14**, no. 1, 2007, pp. 85-105.
[9]. *C. Pfleiderer, H. Petermann,* Strömungsmaschinen, 4th Edition, Springer Verlag, Berlin, 1991.
[10]. *** Fluent 6.0 User's Guide, Fluent Inc., 2001.
[11]. *H.D. Baehr, K. Stephan,* Wärme- und Stoffübertragung, 3rd Edition, Springer-Verlag, Berlin, 1998.